Chemical Engineering Journal 233 (2013) 315–322

Contents lists available at ScienceDirect

Chemical Engineering Journal

journal homepage: www.elsevier.com/locate/cej

A novel chelating resin containing high levels of sulfamine group: Preparation and its adsorption characteristics towards *p*-toluenesulfonic acid and Hg(II)

Yongxin Qi [1], Xinliang Jin [1], Cui Yu, Yang Wang, Liuqing Yang, Yanfeng Li *

State Key Laboratory of Applied Organic Chemistry, Key Laboratory of Nonferrous Metal Chemistry and Resources Utilization of Gansu Province, College of Chemistry and Chemical Engineering, Institute of Biochemical Engineering & Environmental Technology, Lanzhou University, Lanzhou 730000, PR China

HIGHLIGHTS

- The functional monomer with sulfamine (DM-BS) was firstly synthesized.
- The novel adsorbent owned plenty of sulamine prepared by grafting polymerization.
- The resulting adsorbent shows good adsorption for Hg(II) and *p*-toluenesulfonic acid.
- The adsorbent has high selectively separate for Hg(II) and *p*-toluenesulfonic acid.
- The resulting adsorbent has the good regeneration performance.

ARTICLE INFO

Article history:
Received 22 May 2013
Received in revised form 5 August 2013
Accepted 7 August 2013
Available online 14 August 2013

Keywords:
Adsorbent
Solid phase extraction
Selective adsorption
Regeneration
Mercury recovery
p-TSA

ABSTRACT

A novel functional monomers with sulfamine (DM-BS) was prepared by quaternization of N,N-dimethylamino-2-ethyl methacrylate (DMAEMA) and 1-4 bromine methyl toluenesulfonamide (BS-Br). By grafting polymerization of DM-BS onto chloromethylated polystyrene matrix (CMPS), a new kind of adsorbent owned plenty of sulfamine functional group, PSC-DM-P(DM-BS) (PDP), was thereupon synthesized. The resulting DM-BS monomer and PDP adsorbent were characterized by nuclear magnetic resonance spectrum (^{1}H NMR and ^{13}C NMR), Fourier transform infrared spectrum (FT-IR), thermogravimetry (TG) and Elemental analysis. Meanwhile, the adsorption properties of PDP absorbent for Hg(II) and *p*-toluenesulfonic acid (*p*-TSA) in aqueous solution were investigated by batch method. The maximum adsorption capacities for Hg(II) and *p*-TSA were found to be 222.2 mg/g and 312.5 mg/g with the equilibrium time less than 90 min. Furthermore, the PDP absorbent also showed a high selectivity adsorption for Hg(II) among coexisting heavy metals and the good regeneration performance.

1. Introduction

Currently, selectively extracting metal ions and organic pollutants from waste water has stimulated investigation of various possible processes and new materials for water purification caused great interest. Mercury, representation of toxic heavy metals, has been continuously released into the environment and does serious harm to human health [1–5]. The widely used techniques for separation and enrichment of mercury ions are liquid–liquid extraction, ion-exchange, electroanalytical methods, coprecipitation [6–11], etc. And the use of solid phase extraction (SPE) sorbents to separate and preconcentrate metal ions is one of the new developments in the area [12–16]. *p*–toluenesulfonic acid is a kind of very common organic pollutants, heavily polluted of water with rapid industrialization. The method used SPE technique which could remove the mercury heavy metal and *p*-TSA simultaneously, likely the extremely interested means of water treatment for its highly effective and economical property.

Solid phase extraction (SPE), an attractive technique that has commonly been utilized as a technique for separate and preconcentrate of various inorganic and organic pollutants, is considered to be superior to other water purification techniques as regards simplicity, rapidity and ability to attain a high preconcentration factor, high selectivity, stability, etc. [17–20]. Various sorbents including activated carbon [15,20], pure or modified silica gel [13,21], chelating resins and fibers [22–24], etc. have been used in SPE procedures. SPE is used to enhance the selectivity and sensitivity of the method as it allows for discriminatory binding of analyte to a solid support where it will be accumulated and subsequently eluted with a small volume of solvent. Selectivity of the

* Corresponding author. Tel.: +86 93115293104953.
E-mail address: liyf@lzu.edu.cn (Y. Li).
[1] These authors contributed equally to this work.

1385-8947/$ - see front matter © 2013 Elsevier B.V. All rights reserved.
http://dx.doi.org/10.1016/j.cej.2013.08.016

solid phase sorbent towards an adsorbate depends on the structure of the immobilized functional groups [16].

According to Pearson's hard and soft acids and bases theory (HSAB), metal ions will have a preference for complexing with ligands that have more or less electronegative donor atoms. Materials functionalized with sulfur and nitrogen have shown high binding affinity to mercury. There have been many attempts to synthesis solid phase extraction (SPE) sorbents modified with nitrogen and sulfur to purify mercury-contaminated water [25–27]. However, for practical utility there is still a requirement for new materials. In addition, adsorbents containing nitrogen such as amine, hydrazine, thioamide, and imidazoline groups can also adsorb anionic adsorbates through electrostatic interaction [28,29].

Sulfamine functional group, not only shows the high affinity for removal mercury heavy metal, but also has strong adsorption capacity for anionic organic pollutants. Nonetheless, sulfamine modified absorbent has been rarely reported yet. Therefore, in this work, by grafting polymerization the as-prepared monomer that contain sulfamine group onto chloromethylated polystyrene matrix, the novel absorbent which owns numbers of functional group has successfully synthesized. The composition and structure of the resulted absorbent were studied with the help of characterization methods. And it was used as a solid phase extraction sorbents to separate Hg(II) and *p*-TSA from water by batch method. The adsorption models as well as kinetic properties of removal process were also clarified.

2. Experimental part

2.1. Materials

Chloromethylated polystyrene (CMPS) (0.15 mm), 1,2-ethylenediamine, chloroacetate, 1,4-dioxane, N,N-dimethylamino-2-ethyl methacrylate (DMAEMA) (99%, J&K Chemical Ltd.), *p*-Toluenesulfonamide (*p*-TSA) (⩾98%, Tianjin Guangfu Chemical Reagent Co., Ltd.) and N-Bromosuccinimide (NBS) (99%, Tianjin Guangfu Chemical Reagent Co., Ltd.) were used as received. Peroxidation benzoin formyl (BPO) and azobisisobutyronitrile (AIBN) were recrystallized before used. All another chemicals of analytical grade were provided by Tianjin Guangfu Chemical Co., Ltd. and used as received without any further purification.

2.2. Preparation of PSC-DM-P(DM-BS)

2.2.1. Synthesis of monomers DM-BS

The preparation of DM-BS was shown schematically in Fig 1. It was synthesized in two steps. First, 1-4 bromine methyl toluenesulfonamide (BS-Br) was obtained using the following procedure [30]. Put 80 mmol *p*-Toluenesulfonamide, 80 mmol NBS and 2.4 mmo1 BPO into a 500 mL three necks flask, and then 200 mL tetrachloromethane was added. In nitrogen atmosphere, the reaction medium was refluxed for 8 h under continuous mechanical stirring. Thereafter the tetrachloromethane was evaporated, and the residual solid was dissolved in ethyl acetate, washed with saturated salt solution, and extracted with ethyl acetate. The organic layer was dried and a yellow solid was obtained.

Secondly, the monomer, DM-BS, was synthesized by applying the following procedure [31]: Dissolved the DMAEMA (20 mmol) in diethyl ether (50 mL) and added the solution of 20 mmol of BS-Br in acetonitrile (50 ml) at 0 °C. The reaction was stirred for 4 h at 0 °C, and then was left for 16 h at room temperature. The reaction product was filtered off giving a white powder that was washed with diethyl ether and dried under vacuum until constant weight. Yield 43%; m. p., 184–186 °C.

FTIR (KBr, cm^{-1}): 3164 (—OH), 3041 (aromatic C—H), 1729 (C=O), 1416 (C=C—), 1340, 1162 (—SO2—N).1H-NMR (400 MHz, D2O): δ (ppm) 7.96 (d, J = 8.4 Hz, 2H, Hi), 7.70 (d, J = 8.4 Hz, 2 H, Hh), 6.06 (s, 1H, Hb), 5.67 (d, J = 1.6 Hz, 1H, Ha), 4.62 (s, 4H, Hd, Hg), 3.75 (m, 2H, He), 3.08 (s,5H, Hf), 1.84(s,3H, Hj, Hc). 13C-NMR (75 MHz, D2O): δ (ppm) 168.4(Cd), 143.5(Ci), 135.1(Cc), 134.1(Cj), 131.6(Cl), 127.8(Ca), 126.6(Ck), 68.0(Ch), 63.2(Cf), 58.4(Ce), 50.4(Cg), 17.3(Cb). Anal. Calcd. For $C_{15}H_{23}BrN_2O_4S$ (406.06): C, 44.23%; H, 5.69%; N, 6.88%; S, 7.87%. Found: C, 44.16%; H, 5.76%; N, 6.71%; S, 7.69%.

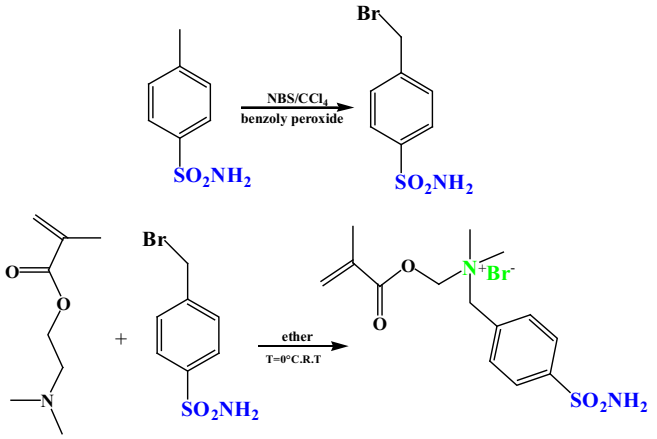

Fig. 1. Synthesis of DM-BS.

2.2.2. Preparation of PSC-DM-P(DM-BS)

In nitrogen atmosphere, 2.00 g of CMPS and 2.0 mL DMAEMA was added into a Schlenk flask with 50 mL diethyl ether in it, the mixture was firstly stirred at 0 °C for 4 h and then stirred for 24 h at room temperature. The reaction product, PSC-DM (PD), was filtered off and washed with acetone. After dried under vacuum, 1.00 g PD was dispersed in 20 ml DMF. Then 0.80 g DM-BS was added and then stirring for 0.5 h under nitrogen atmosphere. After adding 0.08 g AIBN into the solution, the reaction was heated to 80 °C in an oil bath and kept for 6 h. The reaction product PSC-DM-P(DM-BS) (PDP) was filtered off, washed with acetone and ether, then dried under vacuum (Fig. 2).

2.3. Characterization

Proton (1H NMR) and carbon 13 (13C NMR) nuclear magnetic resonance spectra were recorded in a JEOLEX-400 spectrophotometer. The FT-IR spectra of the samples were measured on a pressed pellet with KBr using a Nicolet Magna-IR 550 spectrophotometer. Elemental analyses were carried out using Perkin–Elmer 2400 CHN microanalyser. TGA was conducted with a TA Instruments STA449. The spectrum of the X-ray photoelectron spectroscopy (XPS) of the sample was measured by an X-ray photoelectron spectrometer (VG Scientific Escalab 210-UK) with a twin anode (Mg Kα/Al Kα) source. The HANNA pH meter and a thermo-stated shaker (SHZ-B, China) were used in adsorption batch experiments. The concentrations of ions in solution were determined by a GBC Avanta A 5450 atomic absorption spectrophotometer (AAS), when the selectivity of the adsorbent was studied, an inductively coupled plasma spectrometer (ICP/IRIS Advantage, Thermo, America) was used. The concentration of *p*-TSA was measured by ultraviolet spectrophotometer (UV, TU-1810).

2.4. Adsorption experiments

The selectivity of the adsorbent towards metal ions in mixed system containing Pb(II), Cu(II), Hg(II), Cd(II), Zn(II) and Al(III). The pH of the mixed solution was controlled at pH = 1, at which

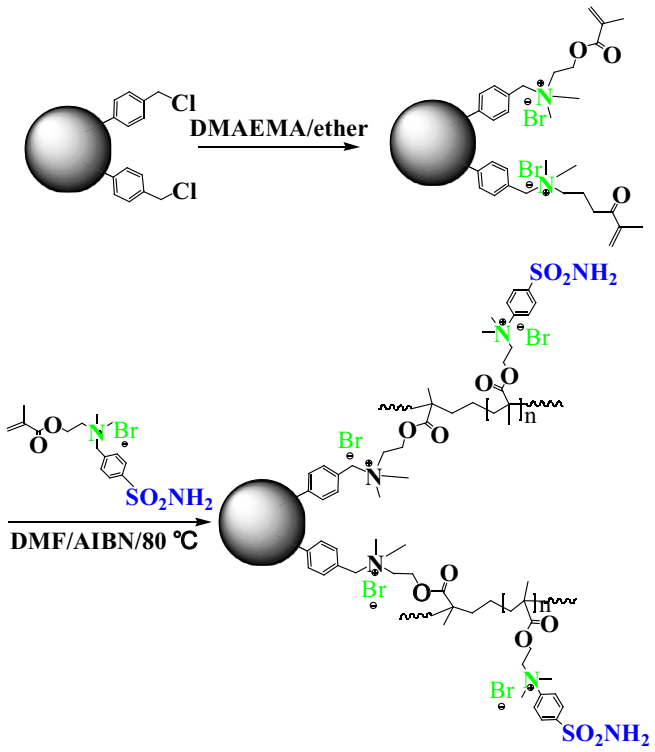

Fig. 2. Synthesis of PSC-DM-P(DM-BS).

pH value the metal ions can exist concurrently. The adsorption experiments were carried out at adsorbent dosages of 2 g/L, shaking in a thermostat oscillator at 120 rpm for a given time. The results are presented in Table 1 and it is obvious that PDP showed a high selectivity to Hg(II) among the coexistent metal ions. Compared with Hg(II), no significant adsorption was observed for other investigated metal ions.

The adsorption potential of this adsorbent for organic pollutants was conducted in the single system. Phenol, benzoic acid, *p*-toluenesulfonic acid, hydroquinone, hydroxyphenol, salicylaldehyde and nitrobenzene were selected as target pollutants. The results showed that the selectivity of PDP for organic pollutant has relationship with the acidity of adsorbate with higher adsorption ability to *p*-toluenesulfonic acid (*p*-TSA) among the studied organic molecules (Table 1).

Therefore, Hg(II) and *p*-TSA was chosen as the inorganic and organic adsorbates, respectively.

The sorption of Hg(II) and *p*-TSA onto the adsorbent was performed in batch experiments. All the adsorption experiments were carried out at adsorbent dosages of 2 g/L, shaking in a thermostated shaker at 120 rpm for a given time. After sorption, the solution was removed and the residual concentration of adsorbate was measured.

The pH of adsorbates solution were adjusted using 0.1 mol/L HNO_3 and NaOH ranging from 1.0 to 6.0 for Hg(II) and 1.0–11.0 for *p*-TSA. Adsorption isotherms and the effects of the initial concentration were studied in the range of 100–2000 ppm for Hg(II) and 50–2280 ppm for *p*-TSA at the optimum pH. The effects of contact time were investigated in the range of 0–25 h for Hg(II) and 0–7 h for *p*-TSA.

3. Results and discussion

3.1. Characterization of PSC-DM-P(DM-BS)

3.1.1. FT-IR spectroscopic analyses

Fig. 3 shows the FTIR spectra of PSC, PD, PDP, meanwhile, the characteristic peaks of each product properly attributed are shown in Table 2. It can be seen from Fig. 3 and Table 2 that the important features peaks of every step product have emerged in the spectrum, suggesting that the synthetic material is the target chelating material.

3.1.2. Element analysis

Table 3 shows the result of elements analysis of PSC and PDP. It can be obviously seen that N and S elements were introduced into PDP material and this could be seen as another proof suggesting the successful synthesis.

3.1.3. TGA analysis

In order to study the thermal stability of the materials, thermo gravimetric analysis (TGA) of PSC, PD, PDP were carried out. From the TGA curve of the PSC, PD, PDP in Fig. 4, no obvious mass loss can be observed in the temperature range of 100–200 °C. It was noted that PSC began to decompose at 320 °C, while PD and PDP began to decompose at about 200 °C, which attributed to the decomposition of DM and P(DM-BS) and several functional groups. The high decomposition temperature indicated that PDP had the excellent thermal stability.

3.2. Adsorption of PDP for Hg(II) and p-TSA

3.2.1. Effect of initial pH

The pH of the adsorbate solution will be deeply effective on the adsorption capacity of the adsorbent. For that, the adsorption of Hg(II) and *p*-TSA were studied in range of 1–6 for Hg(II) and 1–11 for *p*-TSA, and the results were presented in Fig. 5. It is seen that the adsorption of Hg(II) maintained almost the same when the pH ranged from 1 to 4, but increased substantially when the pH value increased from 4 to 6. At low pH value, the protonation of the lone pair of nitrogen could hinder the complex formation, and also have a competitive adsorption between H^+ ions and Hg(II) in the solution, decreased the adsorption capacity [32,33]. With the increase of the pH value, the protonation of nitrogen decrease, resulting in the increase of adsorption capacity of PDP for Hg(II) [34]. However, when pH > 5, the free Hg(II) cations not only interaction with the active sites on the resin but also formation of metal hydroxide species such as soluble $Hg(OH)^+$ and/or insoluble precipitate of $Hg(OH)_2$ [35]. Therefore, the optimum pH for Hg(II) adsorption was chosen as pH = 5.

Table 1
The selectivity of PSC-DM-P(DM-BS) for metal ions and organic pollutants.

PPTS	Pb(II)	Cu(II)	Hg(II)	Cd(II)	Zn(II)	Al(III)	PE	BA	*p*-TSA	HQ	HP	SA	NB
C_0 (mg/L)	100	100	100	100	100	100	100	100	100	100	100	100	100
C_t (mg/L)	95.67	94.8	2.8	100	100	98.4	81.52	27	7.08	78.37	75.45	71.11	67.02
Q (mg/g)	2.165	2.6	48.6	0.00	0.00	0.8	9.24	36.5	46.46	10.815	12.28	14.45	16.49

PE = phenol, BA = benzoic acid, *p*-TSA = *p*-toluenesulfonic acid, HQ = hydroquinone, HP = hydroxyphenol, SA = salicylaldehyde, NB = nitrobenzene.

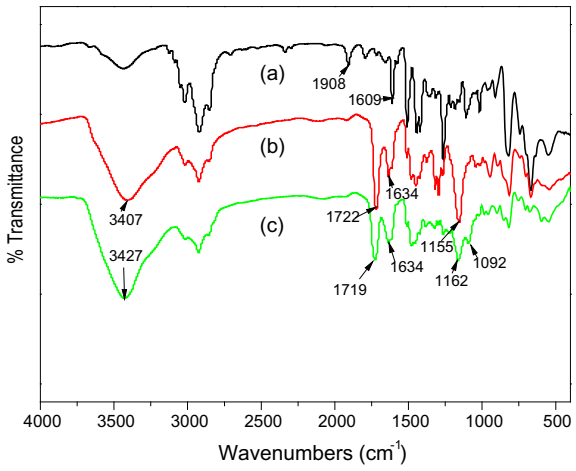

Fig. 3. FTIR spectra of (a) PSC, (b) PSC-DM, and (c) PDP.

Table 2
Characteristics of FT-IR transmission bands of PSC, PSC-DM, PSC-DM-P(DM-BS).

Sample	Band (cm^{-1})	Assignment
PSC	3020	Benzene ring = C—H stretching vibration, υ C—H
	2920, 2851	—CH2— stretching vibration, υ C—H
	1609	C=C— stretching vibration, υ C=C
	822, 669	—C—Cl stretching vibration, υ C—Cl
PSC-DM	1719	C=O stretching vibration, υ C=O
	1634	C=C— stretching vibration, υ C=C
	1319	C—N stretching vibration, υ C—N
	1159	C—O—C stretching vibration, υ C—O
PSC-DM-P(DM-BS)	1160	R—SO2—N— stretching vibration, υ SO2

Table 3
Element analysis of the PSC and PSC-DM-P(DM-BS).

	C%	H%	N%	S%
PSC	77.17	6.738	0	0
PSC-DM-P(DM-BS)	59.86	5.968	2.430	1.842

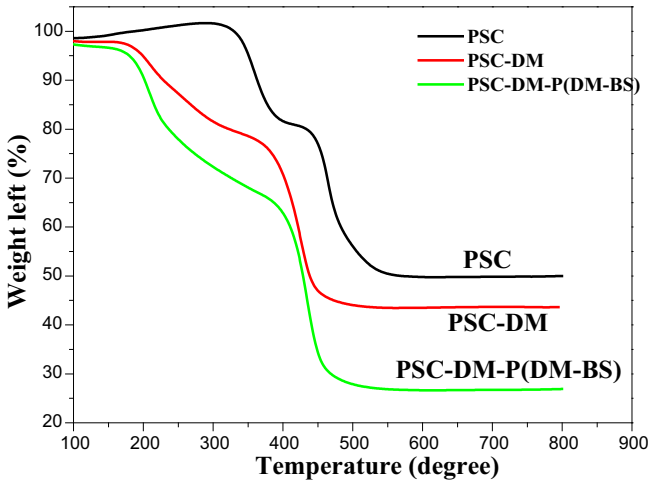

Fig. 4. TGA curves of PSC, PSC-PDM and PDP.

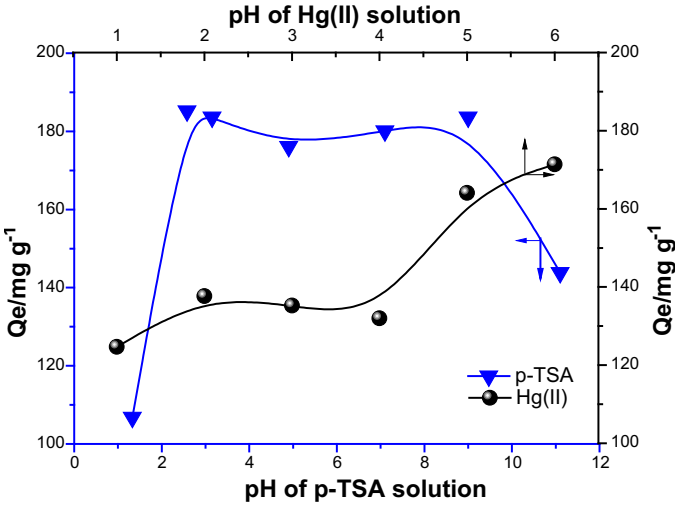

Fig. 5. Effect of pH on adsorption for Hg(II) (C_0 = 500 mg/L) and *p*-TSA adsorption (C_0 = 500 mg/L).

It is conspicuous in Fig. 5 that the adsorption amount of *p*-TSA was basically maintained at the optimum level with the pH range of 2–9. The adsorption of *p*-TSA was caused by two kinds of force: electrostatic interaction and hydrogen bonding actions [16]. At lower pH conditions (below 2), amino groups are protonated and thus result in higher positive surface charge of the PDP adsorbent, and H^+ ions could restrain the dissociation of *p*-TSA, decreasing the electrostatic attraction between *p*-TSA and positively charged absorbent. At higher pH values, OH^- ions may be adsorbed to the surface of PDP adsorbent through a hydrogen bond. The adsorbent surface became negatively charged, so electrostatic attraction between *p*-TSA and positively charged absorbent became weaker, when the pH is high enough electrostatic repulsion occurs between the negative surface charge and *p*-TSA [36].

3.2.2. Effect of sorption time and sorption kinetics

Sorption kinetics was studied to determine the time required to reach the equilibrium. The relationship between reaction time and sorption amounts of Hg(II) and *p*-TSA is presented in Fig. 6. It is noted that Hg(II) and *p*-TSA all reach adsorption equilibrium at 90 min.

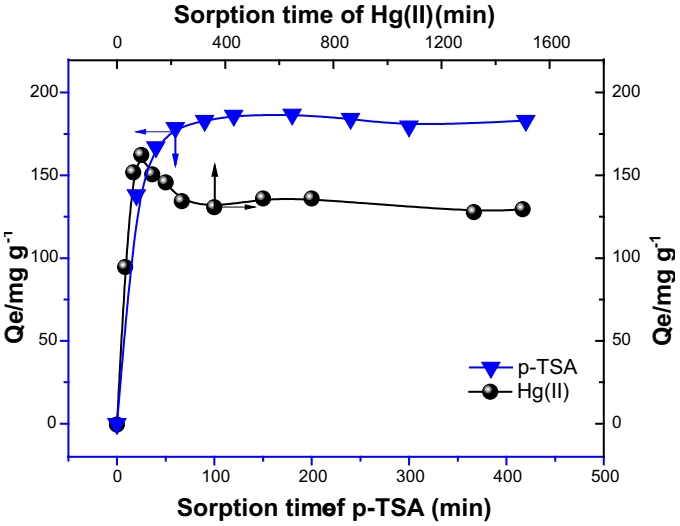

Fig. 6. Effect of shaking time on adsorption of PDP for Hg(II) and *p*-TSA.

The adsorption of *p*-TSA was very rapid with increase of contact time from 0 to 50 min, and reached sorption equilibration at 90 min. This may because that the reaction between acid (*p*-TSA) and base (amino), a kind of anion and cation reaction, was the controlling step which was very fast.

It was found that Hg(II) adsorption reaches a peak at 30 min. There maybe two reasons for the rapid sorption of the material for Hg(II). According to the HSAB theory, Hg(II) was a kind of soft metal and amino belongs to the soft ligand, speed complexation could occur between Hg(II) and material surface functional groups amino. Furthermore, amino could activity flexible distributes in the polymer chain, easy to catch Hg(II). Whereas, decreases after the maximum uptake from 30 min to 60 min. This may be due to the competing adsorption between medium and adsorbate, resulting in incomplete absorption. This kind of medium can improve selectivity during adsorption process, excluding some interference, even though it may be not conducive to the adsorption [37].

The pseudo-first-order and pseudo-second-order kinetic equations were employed to analyze the sorption kinetics of Hg(II) ions and *p*-TSA onto the adsorbent.

The pseudo-first-order (1) and *pseudo-second-order* (2) kinetic model are respectively represented as:

$$\log\ (Q_e - Q_t) = \log\ Q_e - \frac{k_1 t}{2.303} \tag{1}$$

$$\frac{t}{Q_t} = \frac{1}{k_2 Q_e^2} + \frac{t}{Q_e} \tag{2}$$

where k_1 and k_2 are pseudo-first-order rate constant (min^{-1}), pseudo-second-order rate constant ($g\ mg^{-1}\ min^{-1}$) of adsorption, respectively. Q_e and Q_t are the adsorption capacity ($mg\ g^{-1}$) at equilibrium time and at time t (min), respectively.

Figs. 7 and 8 show the curves of t/Q_t versus t and log $(Q_e - Q_t)$ versus t based on the experimental data. The modeled quantitative relationship between times and the sorption process, calculated correlation coefficients are listed in Table 4. From the corresponding parameters summarized in Table 4, it is observed that the kinetic behavior of Hg(II) and *p*-TSA sorption onto the adsorbent is more appropriately described by the pseudo-second-order model because of a much higher correlation coefficient. The pseudo-second-order model was developed based on the assumption that the determining rate step might be chemisorption promoted by covalent forces through the electron exchange or valency forces through electrons sharing between adsorbent and adsorbate,

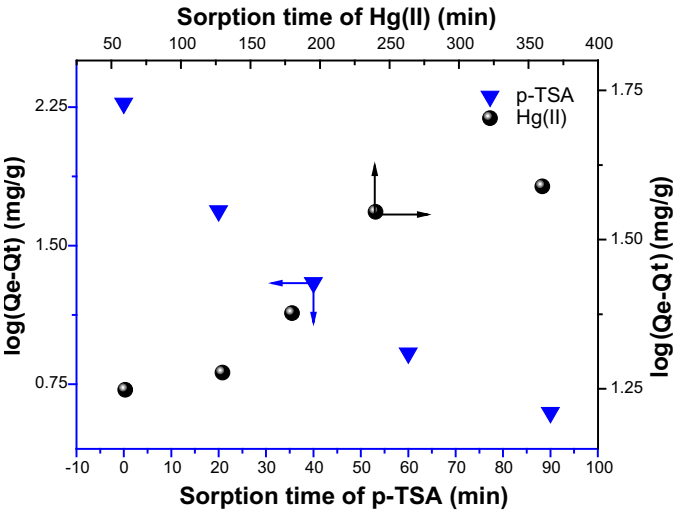

Fig. 7. Pseudo-first-order adsorption kinetics of Hg(II) and *p*-TSA.

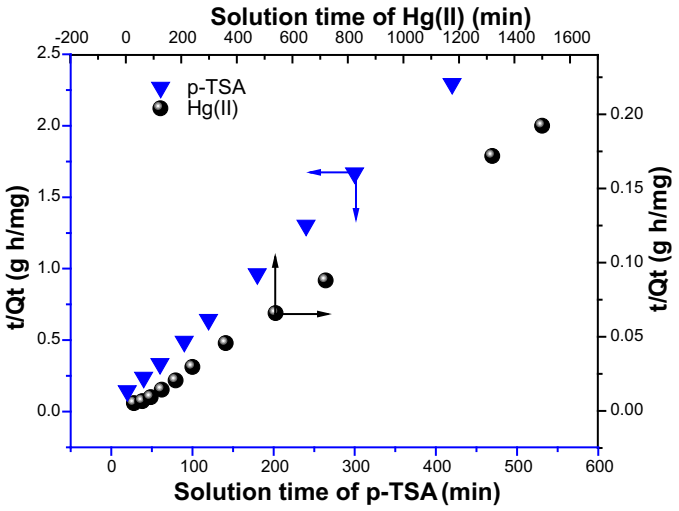

Fig. 8. Pseudo-second-order adsorption kinetics of Hg(II) and *p*-TSA.

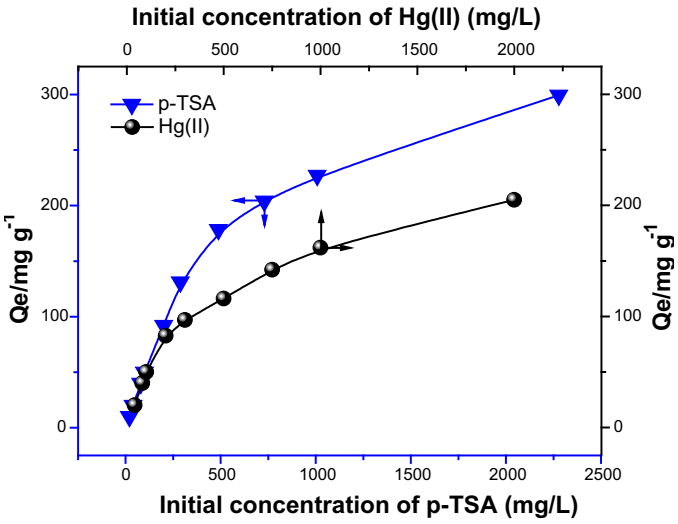

Fig. 9. Effect of initial concentration on Hg(II) and *p*-TSA adsorption.

Table 4
Parameters of kinetic models of Hg(II) and *p*-TSA adsorption onto PDP.

Sample	Pseudo-first-order			Pseudo-second-order		
	Q_{e1} (mg/g)	K_1 (min^{-1})	R_1^2	Q_{e2} (mg/g)	K_2 (g/mg min)	R_2^2
Hg(II)	14.40	0.0030	0.8955	128.2	0.0264	0.9991
p-TSA	134.77	0.0124	0.9645	184.2	0.0025	0.9993

indicating that the behavior of Hg(II) and *p*-TSA sorption onto PDP is mainly the chemically reactive sorption [38].

3.2.3. Effect of initial concentration and sorption isotherm

The effect of the initial concentration on sorption of Hg(II) and *p*-TSA onto the adsorbent was investigated under optimal pH for 3 h, the results are shown in Fig. 9. It appears that the sorption capacity rises significantly with increase in adsorbates concentration. The increase in adsorption capacity may be promoted by the increased drive force, resulting from the concentration variance of adsorbates between solution and the adsorbent. At lower initial adsorbates concentration, abundant active groups on the surface of adsorbent are exposed to adsorbates, resulting in a significantly increase in sorption capacity. Then the sorption process gradually becomes slow with increasing initial concentration.

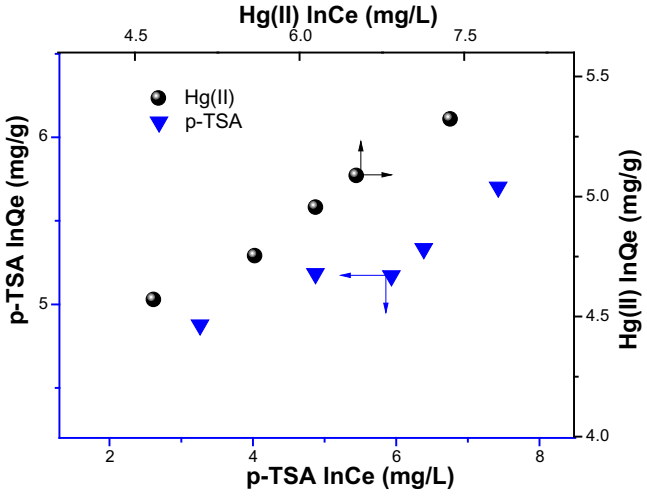

Fig. 10. Freundlich model adsorption isotherms of Hg(II) and *p*-TSA adsorption.

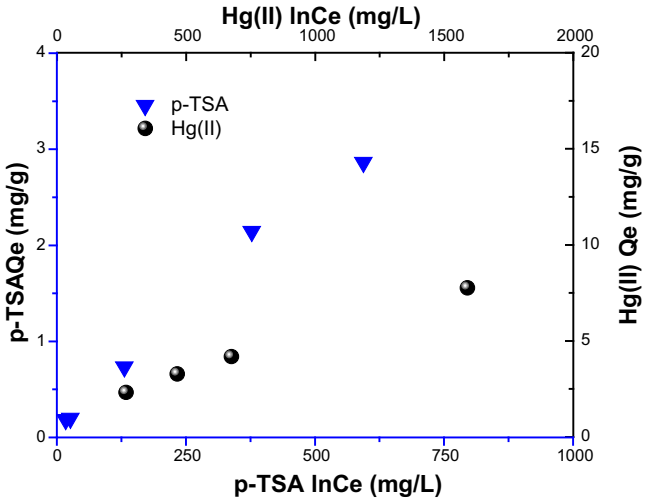

Fig. 11. Langmuir model adsorption isotherms of Hg(II) and *p*-TSA adsorption.

Table 5
Parameters of isotherm model for the adsorption of Hg(II) and *p*-TSA.

Sample		Langmuir			Freundlich		
		Q_{m1} (mg/g)	K_L (L/mg)	R_1^2	K (mg/g) (L/mg)$^{1/n}$	n	R_2^2
PDP	Hg(II)	222.2	0.0057	0.9797	32.50	4.12	0.9688
	p-TSA	312.5	0.0075	0.9646	56.48	4.57	0.9352

Two mathematical models proposed by Freundlich and Langmuir were used to describe and analyze the sorption isotherm of Hg(II) and *p*-TSA. The sorption data in appropriate concentration range were selected to be modeled.

Langmuir equation:

$$\frac{C_e}{Q_e} = \frac{1}{bQ_{\max}} + \frac{C_e}{Q_{\max}} \tag{3}$$

Freundlich equation:

$$\ln\ Q_e = \ln\ K_F + \left(\frac{1}{n}\right) \ln\ C_e \tag{4}$$

where C_e (mg/L) is the concentration of adsorbates solution at equilibrium, Q_e (mg/g) is the amount of sorption at equilibrium. In Langmuir equation, $Q_{\max}$ is the maximum sorption capacity and K_L is Langmuir constant. In Freundlich equation, K and $1/n$ are empirical constants. The modeled quantitative relationship of Hg(II) concentration and *p*-TSA concentration are shown in Figs. 10 and 11 and the calculated correlation coefficients and standard deviations are listed in Table 5. Data in Table 5 point out that the sorption isotherms of Hg(II) and *p*-TSA have all fit Langmuir isotherms, indicating that monolayer chemisorption is the main sorption mechanism. The maximum sorption capacities of PDP for Hg(II) and *p*-TSA were determined as 222.2 mg/g and 312.5 mg/g in the case of monolayer adsorption.

Based on the analysis of the adsorption mechanism of some similar works [43–50], the adsorption mechanism of PDP for metal ions Hg(II) was speculated. The possible mechanism is presented in Fig. 12.

3.2.4. Column adsorption

Column adsorption tests for the absorbents have more meaningful in practical application than the batch experiments. Therefore, we allowed Hg(II) and *p*-TSA solution in each optimum pH condition with initial concentration 200 mg/g to pass through the different column packed with the 0.5 g PDP at 0.5 mL/min to research the column adsorption studies. Fig. 13 shows the breakthrough curves that were plotted as a dimensionless concentration factor C/C_0 (C: the concentration coming out of column and C_0: is the concentration in feed solution) versus effluent volume. The breakthrough curve indicated that the saturation point was achieved when 1900 ml of Hg(II) solution was used, and 2500 ml of *p*-TSA.

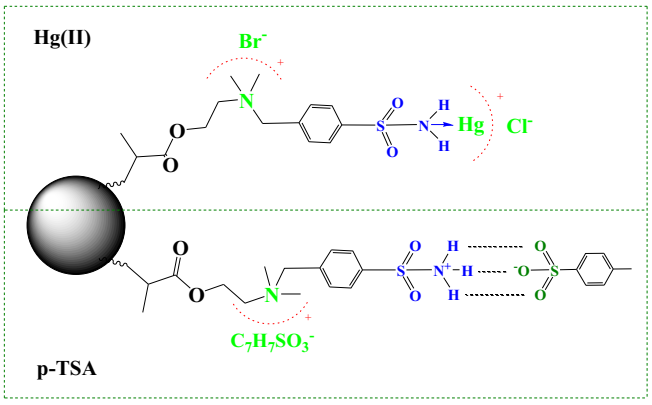

Fig. 12. Scheme of adsorption diagram of the complex formation between PDP and Hg(II)/*p*-TSA.

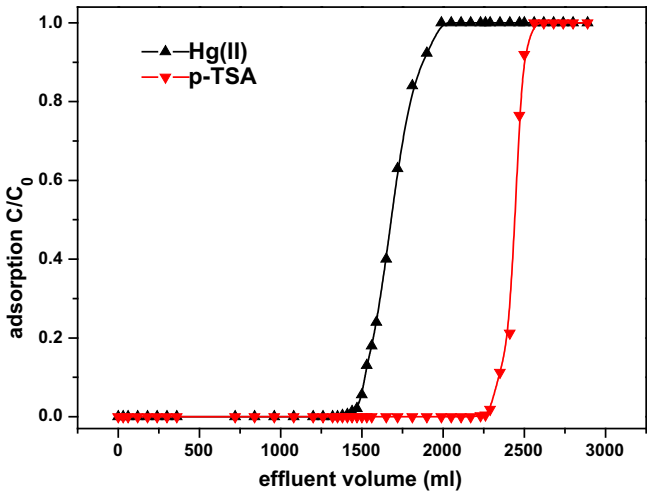

Fig. 13. The breakthrough curve of the PDP.

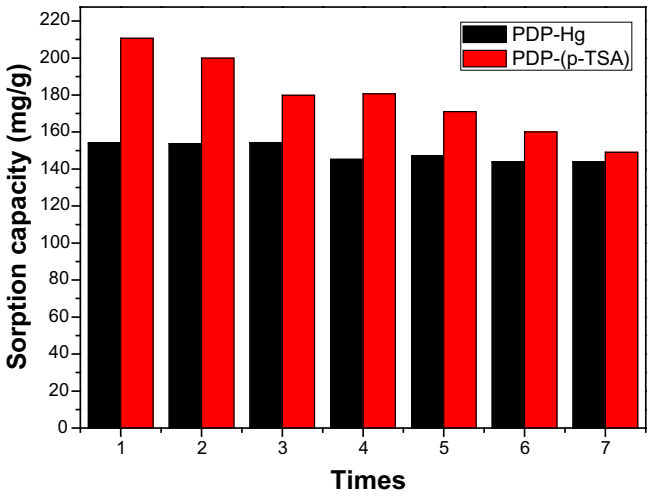

Fig. 16. Repeating adsorption/desorption process with PDP (C_0 Hg(II): 500 mg/l, C_0 *p*-TSA: 1000 mg/l).

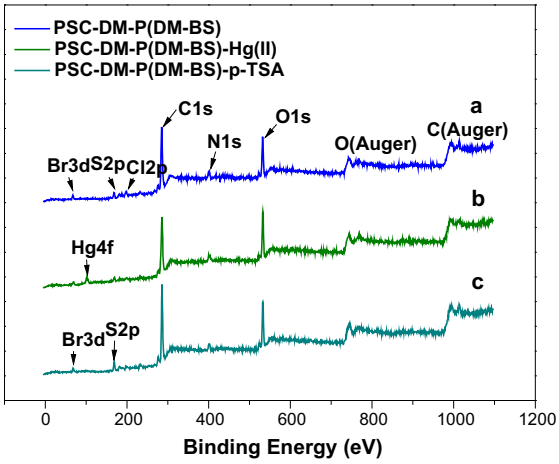

Fig. 14. Typical XPS spectra of PDP: (a) before adsorption (b) after adsorption Hg(II) (c) after adsorption *p*-TSA.

3.2.5. Adsorption mechanism

To provide evidence for adsorption mechanism, XPS was employed. The changes in surface C 1s, O 1s, N 1s, S 2p, Br 3d and Hg 4f element contents are demonstrated by XPS surface analyses of PDP before and after Hg(II), *p*-TSA adsorption (Fig. 14). It can be clearly seen that new peak for Hg 4f after Hg(II) adsorption, and obviously increased the peak for S 2p after *p*-TSA adsorption for PDP.

Fig. 15a shows the XPS N 1s spectra of PDP before and after adsorption. Before adsorption, two major peaks 399.44 eV and 402.23 eV could be attributed to the sulfamine group and N_4^+. After Hg(II) adsorption, the peak of $-SO_2NH_2$ (399.44 eV) increased to 399.69 eV due to the complex with Hg(II), but the peak of N_4^+ cannot be observed obvious change, indicate the N_4^+ almost have no contribution to Hg(II) adsorption. The peak of $-SO_2NH_2$ increased 0.33 eV and the peak of N_4^+ increased 0.22 eV after adsorption for *p*-TSA, demonstrated the basic N atom had strong binding ability for highly acidic *p*-TSA.

Fig. 15b shows the XPS S 2p spectra of PDP before and after adsorption. S atom in $-SO_2NH_2$ group, without long pair of electrons, could not participate the adsorption for Hg(II). The move of the $-SO_2NH_2$ peak may be resulted from electron cloud density decrease which was caused by the chelation between N and Hg(II). No obvious changes have been observed after adsorption for *p*-TSA.

3.2.6. The repeating examination of the batch adsorption

To reduce the cost of removal process, regeneration of the spent adsorbent for repeated reuse is very important. Different

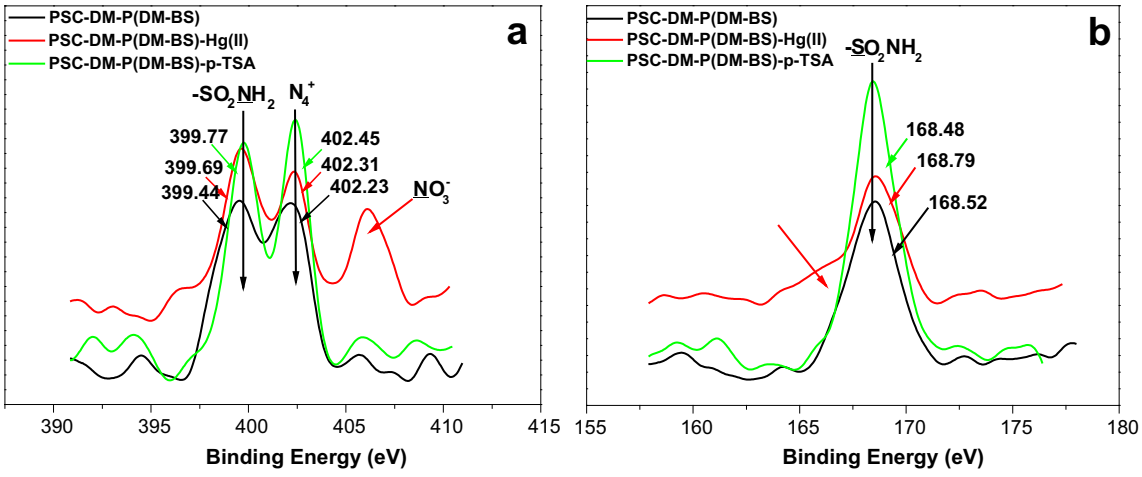

Fig. 15. XPS spectra of PDP before and after adsorption: (a) N 1s spectra (b) S 2p spectra.

concentrations of EDTA, acetic acid, 1M HCl + 10% thiourea and 1M HCl was used for the regeneration of PD*p*-Hg(II), and 1 mol/L NaOH and 0.2 mol/L HCl were used for the regeneration of PD*p*-(*p*-TSA). According to the experiment results, 1M HCl + 10% thiourea and 0.2 mol/L HCl were chosen as the eluents for PD*p*-Hg(II) and PD*p*-(*p*-TSA). The adsorption–desorption cycle of PDP is shown in Fig. 16. The adsorptivity of Hg(II) kept above 95% after seven adsorption–desorption cycles, and the adsorptivity of *p*-TSA drop from 100% to 71% after seven adsorption–desorption cycles. It is obvious that PDP could be utilized repeatedly.

4. Conclusion

In this work, a novel chelating material containing sulfamine PDP was synthesized by polymerization of DM-BS on the surface of chloromethylated polystyrene matrix successively. The synthesized DM-BS monomer was characterized by Proton (1H NMR) and carbon 13 (13C NMR) nuclear magnetic resonance spectra, and PDP was characterized by Fourier transform infrared spectra (FT-IR), thermogravimetry (TG) and Elemental analyses. The adsorption properties of the material for Hg(II) and *p*-TSA were investigated by batch methods. Results show that PDP presented excellent adsorption selectivity adsorption capacity for Hg(II) and *p*-TSA. The adsorption process of Hg(II) and *p*-TSA onto PDP all follow pseudo-second-order kinetics, indicating that chemical adsorption is the rate-controlling step. This work reveals that this material would provide a potential application in the sewage treatment and further scientific development.

Acknowledgements

The authors gratefully acknowledge financial supports from the National Major Specific Program of Science and Technology on Controlling and Administering of Water's pollution (2009ZX07212-001-04), National Training Fund for Talented Person of Basic Subjects (J0730425, J1010067) and the Opening Foundation of State Key Laboratory of Applied Organic Chemistry (SKLAOC-2009-35).

References

[1] J.E. Ferguson, The Heavy Elements: Chemistry, Environmental Impact and Health Effects, Pergamon Press, Oxford, 1990.
[2] X.J. Ma, Y.F. Li, Novel chelating resin with cyanoguanidine group: useful recyclable materials for Hg(II) removal in aqueous environment, J. Hazard. Mater. 185 (2011) 1348–1354.
[3] X.L. Jin, C. Yu, Y.F. Li, Preparation of novel nano-adsorbent based on organic–inorganic hybrid and their adsorption for heavy metals and organic pollutants presented in water environment, J. Hazard. Mater. 186 (2011) 1672–1680.
[4] C.G. Rocha, D.A.M. Zaia, R.V. da Silva Alfaya, A.A. da Silva Alfaya, Use of rice straw as biosorbent for removal of Cu(II), Zn(II), Cd(II) and Hg(II) ions in industrial effluents, J. Hazard. Mater. 166 (2009) 383–388.
[5] A. Khan, S. Badshah, C. Airoldi, Biosorption of some toxic metal ions by chitosan modified with glycidylmethacrylate and diethylenetriamine, Chem. Eng. J. 171 (2011) 159–166.
[6] P.K. Tewari, A.K. Singh, Preconcentration of lead with Amberlite XAD-2 and Amberlite XAD-7 based chelating resins for its determination by flame atomic absorption spectrometry, Talanta 56 (2002) 735–744.
[7] Y.C. Sun, J. Mierzwa, C.R. Lan, Direct determination of molybdenum in seawater by adsorption cathodic stripping square-wave voltammetry, Talanta 52 (2000) 417–424.
[8] U. Divrikli, M. Soylak, L. Elci, Determination of chromium by atomic absorption spectrometry following coprecipitation with cerium (IV) hydroxide. 3rd Mediterranean basin conference on analytical chemistry, Anal. Lett. 145 (2000) 4–9.
[9] B. Alyuz, S. Veli, Kinetics and equilibrium studies for the removal of nickel and zinc from aqueous solutions by ion exchange resins, J. Hazard. Mater. 167 (2009) 482–488.
[10] J. Song, H. Oh, H. Kong, J. Jang, Polyrhodanine modified anodic aluminum oxide membrane for heavy metal ions removal, J. Hazard. Mater. 187 (2011) 311–317.
[11] R. Vinodh, R. Padmavathi, D. Sangeetha, Separation of heavy metals from water samples using anion exchange polymers by adsorption process, Desalination 267 (2011) 267–276.
[12] M. Shamsipur, A.R. Ghiasvand, Y. Yamini, Solid-phase extraction of ultratrace uranium(vi) in natural waters using octadecyl silicamembrane disksmodified by tri-n-octylphosphine oxide and its spectrophotometric determination with dibenzoylmethane, Anal. Chem. 71 (1999) 4892–4895.
[13] R. Laus, T.G. Costa, B. Szpoganicz, V.T. Favere, Adsorption and desorption of Cu(II), Cd(II) and Pb(II) ions using chitosan crosslinked with epichlorohydrin-triphosphate as the adsorbent, J. Hazard. Mater. 183 (2010) 233–241.
[14] S. Sadeghi, E. Sheikhzadeh, Solid phase extraction using silica gel modified with murexide for preconcentration of uranium(VI) ions from water samples, J. Hazard. Mater. 163 (2009) 861–868.
[15] K.P. Desai, Z.V.P. Murthy, Removal of silver from aqueous solutions by complexation–ultrafiltration using anionic polyacrylamide, Chem. Eng. J. 185–186 (2012) 187–192.
[16] G.H. Zhao, Y.F. Li, Preparation of capsules containing 1-nonanol for rapidly removing high concentration phenol from aqueous solution, J. Hazard. Mater. 175 (2010) 715–725.
[17] M.A. Abd, M.H. Mohamed, K.Z. Elwakeel, Adsorption of silver(I) on synthetic chelating polymer derived from 3-amino-1,2,4-triazole-5-thiol and glutaraldehyde, Chem. Eng. J. 151 (2009) 30–38.
[18] Q.F. Lu, M.R. Huang, X.G. Li, Synthesis and heavy-metal-ion sorption of pure sulfophenylenediamine copolymer nanoparticles with intrinsic conductivity and stability, Chem. Eur. J. 13 (2007) 6009–6018.
[19] A.M. Donia, A.A. Atia, F.I. Abouzayed, Preparation and characterization of nano-magnetic cellulose with fast kinetic properties towards the adsorption of some metal ions, Chem. Eng. J. 191 (2012) 22–30.
[20] B. Wen, X.G. Shan, S.G. Xu, Preconcentration oftrace elements in sea water with 8-hydroxyquinoline immobilized polyacrylonitrile hollow fiber membrane for determination by inductively coupled plasmamass spectrometry, Int. J. Environ. Anal. Chem. 77 (2000) 95–109.
[21] I. Narin, M. Soylak, L. Elci, M. Dogan, Separation and enrichment of chromium, copper, nickel and lead in surface seawater samples on column filled with Amberlite XAD-2000, Anal. Lett. 34 (2001) 1935–1947.
[22] S.M.C. Ritchie, K.E. Kissick, L.G. Bachas, S.K. Sikdar, C. Parikh, D. Bhattacharyya, Polycysteine and other polyaminoacid functionalized microfiltration membranes for heavy metal capture, Environ. Sci. Technol. 35 (2001) 3252–3258.
[23] Y. Wang, X.J. Ma, Y.F. Li, X.L. Li, L.Q. Yang, L. Ji, Y. He, Preparation of a novel chelating resin containing amidoxime–guanidine group and its recovery properties for silver ions in aqueous solution, Chem. Eng. J. 209 (2012) 394–400.
[24] X.L. Li, Y.F. Li, Z.F. Ye, Preparation of macroporous bead adsorbents based on poly(vinyl alcohol)/chitosan and their adsorption properties for heavy metals from aqueous solution, Chem. Eng. J. 178 (2011) 60–68.
[25] M. Monier, D.M. Ayad, A.A. Sarhan, Adsorption of Cu(II), Hg(II), and Ni(II) ions by modified natural wool chelating fibers, J. Hazard. Mater. 176 (2010) 348–355.
[26] F.L. Fu, Q. Wang, Removal ions from wastewaters: a review, J. Environ. Manage. 92 (2011) 407–418.
[27] M. Monier, D.A. Abdel-Latif, Preparation of cross-linked magnetic chitosan-phenylthiourea resin for adsorption of Hg(II), Cd(II) and Zn(II) ions from aqueous solutions, J. Hazard. Mater. 209–210 (2012) 240–249.
[28] X.L. Jin, Y.F. Li, C. Yu, Y.X. Ma, H.Y. Hu, Synthesis of novel inorganic–organic hybrid materials for simultaneous adsorption of metal ions and organic molecules in aqueous solution, J. Hazard. Mater. 198 (2011) 247–256.
[29] F. Parra, B. Vazquez, L. Benito, J. Barcenilla, J.S. Roman, Foldable antibacterial acrylic intraocular lenses of high refractive index, Biomacromolecules 10 (2009) 3055–3061.
[30] X. Huang, X. Liao, B. Shi, Hg(II) removal from aqueous solution by bayberry tannin-immobilized collagen fiber, J. Hazard. Mater. 170 (2009) 1141–1148.
[31] A.A. Atia, A.M. Donia, K.Z. Elwakeel, Selective separation of mercury(II) using a synthetic resin containing amine and mercaptan as chelating groups, React. Funct. Polym. 65 (2005) 267–275.
[32] K. Yang, B.S. Xing, Adsorption of fulvic acid by carbon nanotubes from water, Environ. Pollut. 157 (2009) 1095–1100.
[33] F.Z. Bouanis, F. Bentiss, S. Bellayer, J.B. Vogt, C. Jam, Radiofrequency cold plasma nitrided carbon steel: microstructural and micromechanical characterizations, Mater. Chem. Phys. 127 (2011) 329–334.
[34] Y.J. Zhao, Y. Chen, Adsorption of Hg(II) from aqueous solution onto polyacrylamide/attapulgite, J. Hazard. Mater. 171 (2009) 640–646.
[35] B. Benguella, H. Benaissa, Cadmium removal from aqueous solutions by chitin: kinetic and equilibrium studies, Water Res. 36 (2002) 2463–2474.
[36] T.M. Salama, A.H. Ahmed, Z.M. Bahy, Y-type zeolite-encapsulated copper(II) salicylidene-*p*-aminobenzoic Schiff base complex: synthesis, characterization and carbon monoxide adsorption, Micropor. Mesopor. Mater. 89 (2006) 251–259.
[37] B. Dede, F. Karipcin, M. Cengiz, Novel homo- and hetero-nuclear copper(II) complexes of tetradentate Schiff bases: synthesis, characterization, solvent-extraction and catalase-like activity studies, J. Hazard. Mater. 163 (2009) 1148–1156.
[38] J.Z. Zhu, B.L. Deng, J. Yang, Dianchen Gang, Modifying activated carbon with hybrid ligands for enhancing aqueous mercury removal, Carbon 47 (2009) 2014–2025.